Matter perturbations in Galileon cosmology

Antonio De Felice,[1] Ryotaro Kase,[1] and Shinji Tsujikawa[1]

[1]*Department of Physics, Faculty of Science, Tokyo University of Science, 1-3, Kagurazaka, Shinjuku-ku, Tokyo 162-8601, Japan*

(Dated: November 30, 2010)

We study the evolution of matter density perturbations in Galileon cosmology where the late-time cosmic acceleration can be realized by a field kinetic energy. We obtain full perturbation equations at linear order in the presence of five covariant Lagrangians $\mathcal{L}_i$ ($i = 1, \cdots, 5$) satisfying the Galilean symmetry $\partial_\mu\phi \to \partial_\mu\phi + b_\mu$ in the flat space-time. The equations for a matter perturbation as well as an effective gravitational potential are derived under a quasi-static approximation on sub-horizon scales. This approximation can reproduce full numerical solutions with high accuracy for the wavelengths relevant to large-scale structures. For the model parameters constrained by the background expansion history of the Universe the growth rate of matter perturbations is larger than that in the ΛCDM model, with the growth index γ today typically smaller than 0.4. We also find that, even on very large scales associated with the Integrated-Sachs-Wolfe (ISW) effect in Cosmic Microwave Background (CMB) temperature anisotropies, the effective gravitational potential exhibits a temporal growth during the transition from the matter era to the epoch of cosmic acceleration. These properties are useful to distinguish the Galileon model from the ΛCDM in future high-precision observations.

I. INTRODUCTION

The large-distance modification of gravity has received much attention as a possible explanation for the cosmic acceleration today [1]. Many modified gravitational models of dark energy have been already proposed–including those based on $f(R)$ gravity [2], scalar-tensor theories [3], Gauss-Bonnet gravity and its generalizations [4], Dvali-Gabadazde-Porrati (DGP) braneworld [5], and Galileon gravity [6]. In $f(R)$ gravity, for example, the viable models [7] are designed to have a large mass of a scalar gravitational degree of freedom ("scalaron" [8]) in the regions of high density for the compatibility with local gravity experiments. In this case, as long as the so-called chameleon mechanism [9] is at work, the interaction between the scalaron and baryons can be suppressed to satisfy local gravity constraints [10].

There is another mechanism to decouple the fifth force from baryons at short distances even in the absence of the scalar-field potential. Nonlinear effects of field self-interactions can allow the recovery of General Relativity (GR) inside a so-called Vainshtein radius [11]. In the DGP model a longitudinal graviton (i.e. a brane-bending mode ϕ) gives rise to the self-interaction of the form $(r_c^2/m_{\rm pl})\,\Box\phi(\partial^\mu\phi\partial_\mu\phi)$ through the mixing with a transverse graviton, where r_c is a cross-over scale of the order of the Hubble radius H_0^{-1} today and $m_{\rm pl}$ is the Planck mass [12]. In the local region where the energy density ρ is much larger than $r_c^{-2}m_{\rm pl}^2$ the nonlinear self-interaction can lead to the decoupling of the field from matter. However the DGP model suffers from a ghost problem [13], in addition to the difficulty for consistency with the combined data analysis of Supernovae Ia (SN Ia) and Baryon Acoustic Oscillations (BAO) [14].

The self-interacting Lagrangian $\Box\phi(\partial^\mu\phi\partial_\mu\phi)$ appearing in the DGP model satisfies the Galilean symmetry $\partial_\mu\phi \to \partial_\mu\phi + b_\mu$ in the Minkowski background. Imposing the Galilean symmetry in the flat space-time one can show that the field Lagrangian consists of five terms $\mathcal{L}_1, \cdots, \mathcal{L}_5$, where the term $\Box\phi(\partial^\mu\phi\partial_\mu\phi)$ corresponds to $\mathcal{L}_3$ [6]. In Refs. [15] these terms were extended to covariant forms in the curved space-time. Moreover one can keep the equations of motion up to the second-order, while recovering the Galileon Lagrangian in the Minkowski space-time. This property is welcome to avoid the appearance of an extra degree of freedom associated with ghosts.

In Refs. [16, 17] two of the present authors studied the cosmological dynamics of covariant Galileon theory in the presence of the terms up to $\mathcal{L}_5$ (see Refs. [18]-[39] for related works). There exist de Sitter (dS) solutions responsible for dark energy driven by the field kinetic energy. Refs. [16, 17] also clarified the viable model parameter space in which the appearance of ghosts and instabilities of scalar and tensor perturbations can be avoided.

In the covariant Galileon cosmology the solutions finally converge to a common trajectory (tracker), which is characterized by the evolution $\dot{\phi} \propto H^{-1}$ (H is the Hubble parameter) [16]. The epoch at which the solutions approach the tracker depends on the initial conditions of the variable $r_1 \equiv \dot{\phi}_{\rm dS}H_{\rm dS}/(\dot{\phi}H)$, where the subscript "dS" represents the values at the dS point. For smaller initial values of r_1 the approach to the tracker, characterized by $r_1 = 1$, occurs later. In Ref. [40] it was shown that the combined data analysis of SN Ia, BAO, and the CMB shift parameter tends to favor a late-time tracking behavior around the present epoch. This comes from the fact that the dark energy equation of state $w_{\rm DE} \simeq -2$, which corresponds to the one for the tracker during the deep matter era

[16], is difficult to be compatible with a number of observations.

In order to constrain the Galileon model further, it is important to know the evolution of cosmological perturbations from the matter era to the epoch of cosmic acceleration. In particular, the modified growth of matter perturbations δ_m affects the matter power spectrum as well as the weak lensing spectrum [41]. Moreover the modification of gravity manifests itself for the evolution of the effective gravitational potential $\Phi_{\rm eff}$ related with the ISW effect in CMB anisotropies. In this paper we shall derive the equations of cosmological perturbations in the presence of the five Galileon terms $\mathcal{L}_i$ $(i = 1, \cdots, 5)$ and numerically integrate them to find observational signatures of the Galileon model. We also obtain convenient forms of the effective gravitational coupling $G_{\rm eff}$ and the anisotropic parameter η between two gravitational potentials, under a quasi-static approximation for the modes deep inside the Hubble radius.

This paper is organized as follows. In Sec. II we review the Galileon cosmology in the flat Friedmann-Lemaître-Robertson-Walker (FLRW) background. In Sec. III the equations of cosmological perturbations in the Galileon model are derived in the presence of non-relativistic matter. In Sec. IV we obtain the equations for δ_m and $\Phi_{\rm eff}$ under a quasi-static approximation on sub-horizon scales. In Sec. V we present numerical results for the evolution of perturbations by integrating the full equations of motion for the wave numbers relevant to large-scale structures and CMB anisotropies. Sec. VI is devoted to conclusions.

II. BACKGROUND GALILEON COSMOLOGY

Let us consider the following action

$$S = \int {\rm d}^4x\sqrt{-g}\left[\frac{M_{\rm pl}^2}{2}R + \frac{1}{2}\sum_{i=1}^{5} c_i\mathcal{L}_i + p_m(\mu, s)\right], \tag{1}$$

where g is a determinant of the space-time metric $g_{\mu\nu}$, $M_{\rm pl} = (8\pi G)^{-1/2}$ is the reduced Planck mass (with G being gravitational constant), R is a Ricci scalar, and c_i are constants. The five covariant Lagrangians $\mathcal{L}_i$ $(i = 1, \cdots, 5)$ are given by [15]

$$\begin{aligned}
&\mathcal{L}_1 = M^3\phi\,, \quad \mathcal{L}_2 = (\nabla\phi)^2\,, \quad \mathcal{L}_3 = (\Box\phi)(\nabla\phi)^2/M^3\,,\\
&\mathcal{L}_4 = (\nabla\phi)^2\left[2(\Box\phi)^2 - 2\phi_{;\mu\nu}\phi^{;\mu\nu} - R(\nabla\phi)^2/2\right]/M^6,\\
&\mathcal{L}_5 = (\nabla\phi)^2[(\Box\phi)^3 - 3(\Box\phi)\,\phi_{;\mu\nu}\phi^{;\mu\nu} + 2\phi_{;\mu}{}^{\nu}\phi_{;\nu}{}^{\rho}\phi_{;\rho}{}^{\mu} - 6\phi_{;\mu}\phi^{;\mu\nu}\phi^{;\rho}G_{\nu\rho}]/M^9\,,
\end{aligned} \tag{2}$$

where M is a constant having a dimension of mass, and $G_{\nu\rho}$ is the Einstein tensor. These Lagrangians respect the Galilean symmetry in the Minkowski space-time. Moreover the field equations are kept up to the second-order in time derivatives. The last term, p_m, represents the pressure of a perfect fluid whose energy density and equation of state are ρ_m and $w = p_m/\rho_m$, respectively. The pressure depends on a chemical potential $\mu = (\rho_m + p_m)/n$ (n is a number density) and an entropy per particle s.

Since we are interested in the evolution of matter density perturbations long after the radiation-domination, we take into account a non-relativistic fluid ($w \simeq 0$) only in the following discussion. In the FLRW space-time with the scale factor $a(t)$, the variation of the action (2) leads to the background equations [16, 17]:

$$3M_{\rm pl}^2H^2 = \rho_{\rm DE} + \rho_m\,, \tag{3}$$

$$3M_{\rm pl}^2H^2 + 2M_{\rm pl}^2\dot{H} = -p_{\rm DE}\,, \tag{4}$$

where $H = \dot{a}/a$ is the Hubble parameter (a dot represents a derivative with respect to cosmic time t), and

$$\rho_{\rm DE} \equiv -c_1M^3\phi/2 - c_2\dot{\phi}^2/2 + 3c_3H\dot{\phi}^3/M^3 - 45c_4H^2\dot{\phi}^4/(2M^6) + 21c_5H^3\dot{\phi}^5/M^9, \tag{5}$$

$$p_{\rm DE} \equiv c_1M^3\phi/2 - c_2\dot{\phi}^2/2 - c_3\dot{\phi}^2\ddot{\phi}/M^3 + 3c_4\dot{\phi}^3[8H\ddot{\phi} + (3H^2 + 2\dot{H})\dot{\phi}]/(2M^6) - 3c_5H\dot{\phi}^4[5H\ddot{\phi} + 2(H^2 + \dot{H})\dot{\phi}]/M^9. \tag{6}$$

The non-relativistic fluid satisfies the continuity equation $\dot{\rho}_m + 3H\rho_m = 0$.

We shall consider the case in which the late-time cosmic acceleration is realized by the field kinetic terms, i.e. $c_1 = 0$. There is a de Sitter (dS) solution characterized by $H = H_{\rm dS} =$constant and $\dot{\phi} = \dot{\phi}_{\rm dS} =$constant. From Eqs. (3) and (4) it then follows that

$$c_2x_{\rm dS}^2 = 6 + 9\alpha - 12\beta\,, \tag{7}$$

$$c_3x_{\rm dS}^3 = 2 + 9\alpha - 9\beta\,, \tag{8}$$

where $x_{\rm dS} \equiv \dot{\phi}_{\rm dS}/(H_{\rm dS}M_{\rm pl})$ and

$$\alpha \equiv c_4 x_{\rm dS}^4\,, \qquad \beta \equiv c_5 x_{\rm dS}^5\,. \tag{9}$$

We normalize the mass M to be $M^3 = M_{\rm pl}H_{\rm dS}^2$. Since $H_{\rm dS}$ is of the order of the present Hubble parameter ($H_0 \approx 10^{-60}M_{\rm pl}$), we have that $M \approx 10^{-40}M_{\rm pl}$.

In order to discuss the cosmological dynamics, it is convenient to introduce the following variables

$$r_1 \equiv \frac{\dot{\phi}_{\rm dS}H_{\rm dS}}{\dot{\phi}H}\,, \qquad r_2 \equiv \frac{1}{r_1}\left(\frac{\dot{\phi}}{\dot{\phi}_{\rm dS}}\right)^4\,. \tag{10}$$

At the dS point we have $r_1 = 1$ and $r_2 = 1$. The Friedmann equation (3) can be written as $\Omega_{\rm DE} + \Omega_m = 1$, where $\Omega_m \equiv \rho_m/(3M_{\rm pl}^2H^2)$ and

$$\Omega_{\rm DE} \equiv \frac{\rho_{\rm DE}}{3M_{\rm pl}^2H^2} = -\frac{1}{2}(2+3\alpha-4\beta)r_1^3r_2 + (2+9\alpha-9\beta)r_1^2r_2 - \frac{15}{2}\alpha r_1r_2 + 7\beta r_2\,. \tag{11}$$

We also obtain the autonomous equations

$$\begin{aligned} r_1' &= \frac{1}{\Delta}(r_1-1)\,r_1\,[r_1\,(r_1(-3\alpha+4\beta-2)+6\alpha-5\beta)-5\beta] \\ &\quad \times\left[18+3r_2\left(r_1^3(-3\alpha+4\beta-2)+2r_1^2(9\alpha-9\beta+2)-15r_1\alpha+14\beta\right)\right]\,, \qquad (12) \\ r_2' &= -\frac{1}{\Delta}[r_2(6r_1^2(r_2(45\alpha^2-4(9\alpha+2)\beta+36\beta^2)+7(9\alpha-9\beta+2))+r_1^3(-66(3\alpha-4\beta+2) \\ &\quad -3r_2(-2(201\alpha+89)\beta+15\alpha(9\alpha+2)+356\beta^2))-3r_1\alpha(123r_2\beta+36)+10\beta(21r_2\beta-3) \\ &\quad +3r_1^4r_2(9\alpha^2-30\alpha(4\beta+1)+2(2-9\beta)^2)+3r_1^6r_2(3\alpha-4\beta+2)^2+3r_1^5r_2(9\alpha-9\beta+2)(3\alpha-4\beta+2))], \qquad (13) \end{aligned}$$

where a prime represents a derivative with respect to $N = \ln a$, and

$$\begin{aligned} \Delta &\equiv 2r_1^4r_2[72\alpha^2+30\alpha(1-5\beta)+(2-9\beta)^2]+4r_1^2[9r_2(5\alpha^2+9\alpha\beta+(2-9\beta)\beta)+2(9\alpha-9\beta+2)] \\ &\quad +4r_1^3[-3r_2\left(-2(15\alpha+1)\beta+3\alpha(9\alpha+2)+4\beta^2\right)-3\alpha+4\beta-2]-24r_1\alpha(16r_2\beta+3)+10\beta(21r_2\beta+8)\,. \qquad (14) \end{aligned}$$

The Hubble parameter obeys the following equation

$$\frac{H'}{H} = -\frac{5r_1'}{4r_1} - \frac{r_2'}{4r_2}\,. \tag{15}$$

We define the dark energy equation of state $w_{\rm DE}$ and the effective equation of state $w_{\rm eff}$, as

$$w_{\rm DE} \equiv \frac{p_{\rm DE}}{\rho_{\rm DE}}\,, \qquad w_{\rm eff} \equiv -1 - \frac{2H'}{3H}\,. \tag{16}$$

Using the continuity equation $\dot{\rho}_{\rm DE} + 3H(\rho_{\rm DE} + p_{\rm DE}) = 0$, we obtain the relation $w_{\rm DE} = w_{\rm eff} - \Omega_{\rm DE}'/(3\Omega_{\rm DE})$.

There are three distinct fixed points: (A) $(r_1, r_2) = (0, 0)$, (B) $(r_1, r_2) = (1, 0)$, and (C) $(r_1, r_2) = (1, 1)$. As we see from the definition in Eq. (10) the point (C) corresponds to the dS solution, which is always classically stable [17]. The point (B) is a tracker solution found in Ref. [16], along which the field velocity evolves as $\dot{\phi} \propto 1/H$. The fixed point (B) is followed by the stable dS solution once r_2 grows to the order of 1. Depending on the initial conditions of r_1, the epoch at which the solutions approach the tracker is different.

In the following we summarize the background evolution in two regimes: (i) $r_1 \ll 1, r_2 \ll 1$ and (ii) $r_1 = 1$ [16, 17].

- (i) $r_1 \ll 1, r_2 \ll 1$

  This is the regime in which the term $\mathcal{L}_5$ gives the dominant contribution in Eq. (11), i.e.

  $$\Omega_{\rm DE} \simeq 7\beta r_2\,. \tag{17}$$

  Since $r_1' \simeq 9r_1/8$ and $r_2' \simeq 3r_2/8$ from Eqs. (12) and (13), the two variables r_1 and r_2 evolve as

  $$r_1 \propto a^{9/8}\,, \qquad r_2 \propto a^{3/8}\,. \tag{18}$$

During the matter era we have

$$w_{\rm DE} \simeq -1/8\,, \qquad w_{\rm eff} \simeq 0\,. \tag{19}$$

If $\beta r_2 > 0$, then the scalar ghosts do not appear [16, 17]. For the initial conditions with $r_2 > 0$ we require that

$$\beta > 0\,. \tag{20}$$

The conditions for the avoidance of Laplacian instabilities are automatically satisfied [16, 17].

- (ii) $r_1 = 1$

  Along the tracker characterized by $r_1 = 1$, there is a simple relation

$$\Omega_{\rm DE} = r_2\,. \tag{21}$$

  In the regime $r_2 \ll 1$ one has $r_2' \simeq 6r_2$ from Eq. (13), so that the evolution of r_2 during the deep matter era is given by

$$r_2 \propto a^6\,. \tag{22}$$

  Along the tracker the evolution of the Hubble parameter can be analytically known as [40]

$$\left(\frac{H(z)}{H_0}\right)^2 = \frac{1}{2}\Omega_{m0}(1+z)^3 + \sqrt{1-\Omega_{m0}+\frac{(1+z)^6}{4}(\Omega_{m0})^2}\,, \tag{23}$$

  where $z = a_0/a - 1$ is the redshift (a_0 is the scale factor today), and Ω_{m0} is the density parameter of non-relativistic matter today. Even in the presence of radiation and the cosmic curvature there exists an analytic form of $H(z)$ [40].

  Since $\rho_{\rm DE} = 3M^6/H^2$ and $p_{\rm DE} = -3M^6(2+w_{\rm eff})/H^2$, it follows that

$$w_{\rm DE} = -2 - w_{\rm eff} = -\frac{2}{r_2+1}\,, \qquad w_{\rm eff} = -\frac{2r_2}{r_2+1}\,. \tag{24}$$

  In the deep matter era ($r_2 \ll 1$) we have $w_{\rm DE} = -2$ and $w_{\rm eff} = 0$, whereas at the dS solution $w_{\rm DE} = w_{\rm eff} = -1$. The conditions for the avoidance of ghosts and Laplacian instabilities have been derived in Refs. [16, 17]. The allowed parameter space in the (α, β) plane is summarized in figure 1 of Ref. [16].

It should be pointed out that the tracker solution and the $\mathcal{L}_5$-dominant solution can be distinguished also by means of the following physical quantity. When $c_1 = 0$ one has $\partial L/\partial\phi = 0$, where $L \equiv \sqrt{-g}\mathcal{L}$ is the Lagrangian including the volume factor $\sqrt{-g}$ in Eq. (1). Then the conjugate momentum to the field ϕ is conserved, so that $\partial L/\partial\dot{\phi} =$ constant. This constraint can be written as

$$P_\phi \equiv \frac{{r_2}^{1/4}\, a^3\,(1-r_1)\left(2\,{r_1}^2 + 3\alpha\,{r_1}^2 - 4\beta\,{r_1}^2 - 6\,\alpha\,r_1 + 5\beta\,r_1 + 5\,\beta\right)}{{r_1}^{11/4}} = \text{constant}\,. \tag{25}$$

On the tracker P_ϕ exactly vanishes[1], whereas for the $\mathcal{L}_5$-dominant solution $P_\phi \simeq 5\beta\, a^3\,(r_2/r_1^{11})^{1/4} \neq 0$. Although Eq. (25) is not independent of the others, we will use it later on in order to check the good convergence of numerical solutions.

III. COSMOLOGICAL PERTURBATIONS

Let us consider scalar metric perturbations Ψ, Φ, and χ about the flat FLRW background [42]:

$$ds^2 = -(1+2\Psi)dt^2 - 2a(t)\partial_i\chi dt dx^i + a^2(t)(1+2\Phi)\delta_{ij}dx^i dx^j\,, \tag{26}$$

[1] The tracker can then be seen as the zero momentum solutions.

where we have chosen the spatial gauge such that the spatial metric is diagonal. There is still a freedom to fix the temporal part ξ_0 of a vector associated with a scalar gauge transformation. Later on we will discuss this gauge degree of freedom in more detail.

The field ϕ is decomposed into the background and inhomogeneous parts, as $\phi(t, \boldsymbol{x}) = \tilde{\phi}(t) + \delta\phi(t, \boldsymbol{x})$. In the following we omit the tilde for the background quantity. For the perfect fluid, we cannot set $w = 0$ in Eq. (1) identically from the beginning as its action would vanish. However, we can consider a fluid whose equation of state parameter w is different from zero, and only after we obtain the equations of motion for the perturbation variables, we will take the limit $w \to 0$. Since we are interested in the scalar perturbations of a cold fluid (temperature $T = 0$) with a barotropic equation of state of the form $p_m = w\rho_m$ (in the limit $w \to 0$), the action approach of linear perturbation theory for a perfect fluid introduced in Refs. [43] can be simplified as follows.

Let us define a 4-velocity of the perfect fluid, as $u_\alpha = \mu^{-1}\,\partial_\alpha \ell$. The normalization of the 4-velocity ($u_\alpha u^\alpha = -1$) implies that $\mu = \sqrt{-g^{\alpha\beta}\partial_\alpha\ell\partial_\beta\ell}$. Then at linear level we have $\delta\mu = -\dot{\delta\ell} - \mu\Psi$. Now the quantity $\sqrt{-g}\,p_m(\mu, s)$ can be expanded at second order in the gravitational fields and in $\delta\ell$ and δs. However, since the fluid is cold ($T = 0$), the first principle of thermodynamics, $\mathrm{d}p_m = n\mathrm{d}\mu - nT\mathrm{d}s$, imposes that $(\partial p_m/\partial s)_\mu$, $(\partial^2 p_m/\partial s^2)_\mu$, and $(\partial^2 p_m/\partial s\partial\mu)$ vanish[2]. In turn this implies that p_m depends on μ alone, and we do not need to expand the action in terms of δs, the entropy perturbation field[3]. Furthermore, since $\rho_m \equiv n\mu - p_m$, it follows that $\mathrm{d}\rho_m = \mu\,\mathrm{d}n + nT\mathrm{d}s = \mu\,\mathrm{d}n = \mu\dot{n}\,\delta\mu/\dot{\mu}$ at linear level. Using the field redefinition $\delta\ell = -\mu v$, where v is a velocity potential for the perfect fluid, after some algebra, we find

$$\dot{v} - 3Hwv = \Psi + \frac{w}{1+w}\delta\,, \tag{27}$$

where $\delta \equiv \delta\rho_m/\rho_m$ is the density contrast.

In Fourier space the density contrast obeys the following equation of motion [44]

$$\dot{\delta} = -(1+w)\left(3\dot{\Phi} + \frac{k^2}{a^2}v - \frac{k^2}{a^2}\,\chi\right)\,, \tag{28}$$

where k is a comoving wave number. This equation follows from the first-order part of the continuity equation $\nabla_\mu T^\mu_0 = 0$. In the following we derive other perturbation equations from the second-order action for perturbations. In Appendix A we will show how to obtain Eq. (28) from the action approach.

Let us consider non-relativistic matter with $w = 0$. We introduce the gauge-invariant matter perturbation δ_m, as [42]

$$\delta_m \equiv \delta + 3Hv\,. \tag{29}$$

Using Eqs. (28) and (27), it follows that

$$\ddot{\delta}_m + 2H\dot{\delta}_m + \frac{k^2}{a^2}\Psi = 3(\ddot{Q} + 2H\dot{Q})\,, \tag{30}$$

where $Q \equiv Hv - \Phi$.

Let us now derive the coupled equations for metric/field/matter perturbations. Expansion of the action (1) at second order gives

$$[\sqrt{-g}\mathcal{L}]^{(2)} \equiv L(\Psi, \Phi, \chi, \delta\phi, v)\,. \tag{31}$$

If we vary the Lagrangian (31) with respect to Ψ, then we find a term $\rho_m(\Psi - \dot{v})/w$ that leads to an apparent singularity for $w \to 0$. However, Eq. (27) allows to reduce this term to $-\rho_m[\delta/(1+w) + 3Hv]$. Taking the limit $w \to 0$ at the end, we obtain the equation of motion

$$E_\Psi \equiv A_1\dot{\Phi} + A_2\dot{\delta\phi} - \rho_m\dot{v} + A_3\frac{k^2}{a^2}\Phi + A_4\Psi + A_5\frac{k^2}{a^2}\chi + \left(\frac{1}{2}c_1M^3 + A_6\frac{k^2}{a^2}\right)\delta\phi - \rho_m\delta = 0\,, \tag{32}$$

where the coefficients A_i are given in Appendix B.

---

[2] This also implies that $n = n(\mu)$. For example, $\mu \propto n^w$ is enough to give $p_m = w\rho_m$.

[3] In the equations of motion approach, this result corresponds to the fact that, once $p_m = w\rho_m$, no entropy perturbations appear in the dynamical equations.

Variations of the second-order Lagrangian L with respect to Φ, χ, and $\delta\phi$ result in the following equations

$$E_\Phi \equiv B_1\ddot{\Phi} + B_2\ddot{\delta\phi} + B_3\dot{\Phi} + B_4\dot{\delta\phi} + B_5\dot{\Psi} + B_6\frac{k^2}{a^2}\Phi + \left(B_7\frac{k^2}{a^2} + \frac{3}{2}c_1M^3\right)\delta\phi + \left(B_8\frac{k^2}{a^2} + B_9\right)\Psi + B_{10}\frac{k^2}{a^2}\dot{\chi} + B_{11}\frac{k^2}{a^2}\chi + 3\rho_m\dot{v} = 0\,, \tag{33}$$

$$E_\chi \equiv C_1\dot{\Phi} + C_2\dot{\delta\phi} + C_3\Psi + C_4\delta\phi + \rho_m v = 0\,, \tag{34}$$

$$E_{\delta\phi} \equiv D_1\ddot{\Phi} + D_2\ddot{\delta\phi} + D_3\dot{\Phi} + D_4\dot{\delta\phi} + D_5\dot{\Psi} + D_6\frac{k^2}{a^2}\dot{\chi} + \left(D_7\frac{k^2}{a^2} + D_8\right)\Phi + D_9\frac{k^2}{a^2}\delta\phi + \left(D_{10}\frac{k^2}{a^2} + D_{11}\right)\Psi + D_{12}\frac{k^2}{a^2}\chi = 0\,, \tag{35}$$

where the coefficients B_i, C_i, and D_i are given in Appendix B. Varying the Lagrangian L in terms of v gives rise to Eq. (27), i.e. $\dot{v} = \Psi$ for $w = 0$.

Another constraint equation can be found by introducing the perturbation γ in the metric (26), as $\delta g_{ij} = 2a^2\partial_i\partial_j\gamma$. Its equation of motion is given by

$$E_\gamma \equiv \frac{1}{3}(B_1\ddot{\Phi} + B_2\ddot{\delta\phi} + B_3\dot{\Phi} + B_4\dot{\delta\phi} + B_5\dot{\Psi} + B_9\Psi) + \frac{1}{2}c_1M^3\delta\phi + \rho_m\dot{v} = 0\,, \tag{36}$$

which does not contain γ explicitly (as the quadratic terms in γ in the action can be integrated out). Evaluating $E_\Phi - 3E_\gamma$ leads to the following equation

$$\tilde{E}_\gamma \equiv B_6\,\Phi + B_7\,\delta\phi + B_8\,\Psi + B_{10}\,\dot{\chi} + B_{11}\,\chi = 0\,. \tag{37}$$

The same relation can be derived by using the Bianchi identities, see Appendix A.

In what follows we choose the longitudinal gauge with $\chi = 0$. This choice, together with imposing $\gamma = 0$, completely fixes the gauge. We also set $c_1 = 0$ to discuss the evolution of cosmological perturbations.

IV. QUASI-STATIC APPROXIMATION ON SUB-HORIZON SCALES

Let us consider the evolution of perturbations for the modes deep inside the Hubble radius. We derive the equations of matter perturbations and gravitational potentials under the quasi-static approximation on sub-horizon scales ($k \gg aH$). This corresponds to the approximation under which the dominant contributions to the perturbation equations are those including k^2/a^2 and δ [45, 46]. In the longitudinal gauge we obtain the following approximate equations from Eqs. (32), (37), and (35):

$$\frac{k^2}{a^2}\left(A_3\Phi + A_6\delta\phi\right) \simeq \rho_m\delta\,, \tag{38}$$

$$B_6\Phi + B_7\delta\phi + B_8\Psi = 0\,, \tag{39}$$

$$D_7\Phi + D_9\delta\phi + D_{10}\Psi \simeq 0\,. \tag{40}$$

From Eqs. (39) and (40) one can express Φ and $\delta\phi$ in terms of Ψ, i.e.

$$\Phi \simeq \frac{A_3D_9 - A_6B_7}{B_7^2 - B_6D_9}\Psi\,, \tag{41}$$

$$\delta\phi \simeq \frac{A_6B_6 - A_3B_7}{B_7^2 - B_6D_9}\Psi\,, \tag{42}$$

where we have used $B_8 = A_3$, $D_7 = B_7$, and $D_{10} = A_6$. Substituting Eqs. (41) and (42) into Eq. (38), it follows that

$$\frac{k^2}{a^2}\Psi \simeq -4\pi G_{\rm eff}\rho_m\delta\,, \tag{43}$$

where

$$G_{\rm eff} \equiv \frac{2M_{\rm pl}^2(B_7^2 - B_6D_9)}{2A_3A_6B_7 - A_3^2D_9 - A_6^2B_6}G\,. \tag{44}$$

Since $|\dot{\delta}|$ is at most of the order of $|H\delta|$ in Eq. (28), one has $|(k^2/a^2)v| \lesssim |H\delta|$. This means that $|Hv/\delta| \lesssim (aH/k)^2 \ll 1$ for sub-horizon modes, which leads to $\delta_m \simeq \delta$ in Eq. (29). Since the r.h.s. of Eq. (30) can be neglected relative to the l.h.s., we obtain the equation for the gauge-invariant matter perturbation for the modes deep inside the Hubble radius:

$$\ddot{\delta}_m + 2H\dot{\delta}_m - 4\pi G_{\rm eff}\rho_m\delta_m \simeq 0\,, \tag{45}$$

where we have used the Poisson equation (43).

From Eqs. (42) and (43) the field perturbation is given by

$$\delta\phi \simeq \frac{3M_{\rm pl}^2(A_3B_7 - A_6B_6)}{2A_3A_6B_7 - A_3^2D_9 - A_6^2B_6}\left(\frac{aH}{k}\right)^2\Omega_m\delta\,. \tag{46}$$

We introduce the following quantity to describe the difference between the two gravitational potentials:

$$\eta \equiv -\frac{\Phi}{\Psi} \simeq \frac{A_3D_9 - A_6B_7}{B_6D_9 - B_7^2}\,, \tag{47}$$

where we have used Eq. (41) in the last approximate equality. We also define the effective gravitational potential

$$\Phi_{\rm eff} \equiv (\Psi - \Phi)/2\,, \tag{48}$$

which is related with the deviation of the light rays in CMB and weak lensing observations [41]. From the Poisson equation (43) it follows that

$$\frac{k^2}{a^2}\Phi_{\rm eff} \simeq -4\pi G_{\rm eff}\frac{1+\eta}{2}\rho_m\delta\,. \tag{49}$$

Using the density parameter $\Omega_m = 8\pi G\rho_m/(3H^2)$ and the relation $\delta_m \simeq \delta$, we have

$$\Phi_{\rm eff} \simeq -\frac{3}{2}\frac{G_{\rm eff}}{G}\frac{1+\eta}{2}\Omega_m\delta_m\left(\frac{aH}{k}\right)^2\,. \tag{50}$$

The matter perturbation equation (45) can be written as

$$\delta_m'' + \left(2 + \frac{H'}{H}\right)\delta_m' - \frac{3}{2}\frac{G_{\rm eff}}{G}\Omega_m\delta_m \simeq 0\,. \tag{51}$$

In the limit that $\dot{\phi} \to 0$ and $\ddot{\phi} \to 0$, the effective gravitational coupling $G_{\rm eff}$ reduces to G. Hence, in the early cosmological epoch, the General Relativistic behavior is recovered. If $G_{\rm eff} \simeq G$, then the evolution of matter perturbations during the deep matter era ($H'/H \simeq -3/2$ and $\Omega_m \simeq 1$) is given by $\delta_m \propto a \propto t^{2/3}$.

As the field velocity grows in time, $G_{\rm eff}$ is subject to change. This leads to the modified growth rate of matter perturbations compared to the ΛCDM model. Unlike $f(R)$ gravity [46] and Brans-Dicke theory [47] the effective gravitational coupling is independent of the wave number k. The quantity η defined in Eq. (47) reduces to 1 for $\dot{\phi} \to 0$ and $\ddot{\phi} \to 0$, but it deviates from 1 with the growth of $\dot{\phi}$ and $\ddot{\phi}$. In three different regimes characterized by (i) $r_1 \ll 1$, $r_2 \ll 1$, (ii) $r_1 = 1$, $r_2 \ll 1$, and (iii) $r_1 = 1$, $r_2 = 1$, one can estimate $G_{\rm eff}$ and η as follows.

- (i) $r_1 \ll 1$, $r_2 \ll 1$

  In this case we expand $G_{\rm eff}$ and η about $r_1 = 0, r_2 = 0$. Together with the use of the background equations (12) and (13), we obtain

$$\frac{G_{\rm eff}}{G} = 1 + \left(\frac{255}{8}\beta + \frac{211}{16}\alpha r_1\right)r_2 + \mathcal{O}(r_2^2)\,, \tag{52}$$

$$\eta = 1 + \left(\frac{129}{8}\beta + \frac{589}{16}\alpha r_1\right)r_2 + \mathcal{O}(r_2^2)\,. \tag{53}$$

  In this epoch the cosmological dynamics is dominated by the term $\mathcal{L}_5$. Since $\beta > 0$ to avoid ghosts, we have that $G_{\rm eff} > G$ and $\eta > 1$ in this regime. Hence the growth rates of δ_m and $\Phi_{\rm eff}$ are larger than those in the ΛCDM model.

- (ii) $r_1 = 1$, $r_2 \ll 1$

  Expanding $G_{\rm eff}$ and η about $r_2 = 0$, it follows that

$$\frac{G_{\rm eff}}{G} = 1 + \frac{291\alpha^2 + 702\beta^2 - 933\alpha\beta + 20\alpha - 84\beta + 4}{2(10\alpha - 9\beta + 8)} r_2 + \mathcal{O}(r_2^2)\,, \tag{54}$$

$$\eta = 1 - \frac{3(126\alpha^2 + 306\beta^2 - 405\alpha\beta + 4\alpha - 30\beta)}{2(10\alpha - 9\beta + 8)} r_2 + \mathcal{O}(r_2^2)\,. \tag{55}$$

  The evolution of $G_{\rm eff}$ and η depends on both α and β. If $\alpha = 1.4$ and $\beta = 0.4$, for example, we have $G_{\rm eff}/G \simeq 1 + 4.31 r_2$ and $\eta \simeq 1 - 5.11 r_2$, respectively. In this case $G_{\rm eff} > G$, but η is smaller than 1.

- (iii) $r_1 = 1$, $r_2 = 1$

  At the dS point we have

$$\frac{G_{\rm eff}}{G} = \frac{1}{3(\alpha - 2\beta)}\,, \tag{56}$$

$$\eta = 1\,. \tag{57}$$

  This means that η is not subject to change compared to the ΛCDM model. In Refs. [16, 17] it was shown that the viable parameter space consistent with the absence of ghosts and instabilities is confined in the region $2\beta \leq \alpha \leq 2\beta + 2/3$. From Eq. (56) the effective gravitational coupling is constrained to be $G_{\rm eff}/G \geq 1/2$. On the line $\alpha = 2\beta$, $G_{\rm eff}$ goes to infinity (this includes the case in which only the terms up to $\mathcal{L}_3$ are present, i.e. $\alpha = \beta = 0$). On the line $\alpha - 2\beta = 1/3$, the effective gravitational coupling is equivalent to G.

The above approximate formulas are useful to discuss the evolution of perturbations on the scales relevant to large-scale structures.

V. NUMERICAL RESULTS

In this section we present numerical results for the evolution of perturbations without employing the quasi-static approximation on sub-horizon scales. The accuracy of the quasi-static approximation will be confirmed for the modes $k \gg aH$.

Among the six equations (32)-(37), three of them are independent. For the numerical purpose we solve Eqs. (32), (34), and (37) together with Eqs. (27) and (28). We have also confirmed that P_ϕ defined in Eq. (25) remains constant up to the accuracy of 10^{-8} during the whole evolution. It is convenient to introduce the following dimensionless variables

$$V \equiv Hv\,, \qquad \delta\varphi \equiv \delta\phi/(x_{\rm dS} M_{\rm pl})\,, \tag{58}$$

with $\tilde{A}_1 \equiv A_1/(HM_{\rm pl}^2)$, $\tilde{A}_2 \equiv x_{\rm dS}A_2/(HM_{\rm pl})$, $\tilde{A}_3 \equiv A_3/M_{\rm pl}^2$, $\tilde{A}_4 \equiv A_4/(H^2M_{\rm pl}^2)$, $\tilde{A}_6 \equiv x_{\rm dS}A_6/M_{\rm pl}$, $\tilde{B}_6 \equiv B_6/M_{\rm pl}^2$, $\tilde{B}_7 \equiv x_{\rm dS}B_7/M_{\rm pl}$, and $\tilde{C}_4 \equiv x_{\rm dS}C_4/(HM_{\rm pl})$. In the longitudinal gauge we obtain the following equations from Eqs. (32), (34), (37), (28), and (27):

$$\Psi = -(\tilde{B}_6\Phi + \tilde{B}_7\delta\varphi)/A_3\,, \tag{59}$$

$$\begin{aligned}\Phi' = {} & [(3\tilde{A}_4\tilde{A}_6\tilde{B}_6 + \tilde{A}_1\tilde{A}_2\tilde{B}_6 - 3\tilde{A}_3^2\tilde{A}_6k^2/(aH)^2 - 9\tilde{A}_6\tilde{B}_6\Omega_m)\Phi \\ & +(3\tilde{A}_2\tilde{A}_3\tilde{C}_4 + 3\tilde{A}_4\tilde{A}_6\tilde{B}_7 + \tilde{A}_1\tilde{A}_2\tilde{B}_7 - 9\tilde{A}_6\tilde{B}_7\Omega_m - 3\tilde{A}_3\tilde{A}_6^2k^2/(aH)^2)\delta\varphi + 9\tilde{A}_3\tilde{A}_6\Omega_m\delta + 9\tilde{A}_2\tilde{A}_3\Omega_m V] \\ & \times[3\tilde{A}_3(\tilde{A}_1\tilde{A}_6 - \tilde{A}_2\tilde{A}_3)]^{-1}\,,\end{aligned} \tag{60}$$

$$\begin{aligned}\delta\varphi' = {} & -[(\tilde{A}_1^2\tilde{B}_6 + 3\tilde{A}_3\tilde{A}_4\tilde{B}_6 - 3\tilde{A}_3^3k^2/(aH)^2 - 9\tilde{A}_3\tilde{B}_6\Omega_m)\Phi \\ & +(\tilde{A}_1^2\tilde{B}_7 + 3\tilde{A}_3\tilde{A}_4\tilde{B}_7 + 3\tilde{A}_1\tilde{A}_3\tilde{C}_4 - 3\tilde{A}_3^2\tilde{A}_6k^2/(aH)^2 - 9\tilde{A}_3\tilde{B}_7\Omega_m)\delta\varphi + 9\tilde{A}_3^2\Omega_m\delta + 9\tilde{A}_1\tilde{A}_3\Omega_m V] \\ & \times[3\tilde{A}_3(\tilde{A}_1\tilde{A}_6 - \tilde{A}_2\tilde{A}_3)]^{-1}\,,\end{aligned} \tag{61}$$

$$\delta' = -3\Phi' - k^2/(aH)^2\, V\,, \tag{62}$$

$$V' = (H'/H)V + \Psi\,, \tag{63}$$

where we have used $\tilde{B}_8 = \tilde{A}_3$, $\tilde{C}_1 = \tilde{A}_3$, $\tilde{C}_2 = \tilde{A}_6$, and $\tilde{C}_3 = -\tilde{A}_1/3$. The time-dependent coefficients $\tilde{A}_1$, $\tilde{B}_6$, e.t.c. can be expressed by using the variables α, β, r_1, and r_2. Solving the perturbation equations (59)-(63) together with the background equations (12) and (13), we find the evolution of Ψ, Φ, $\delta\varphi$, δ, and V.

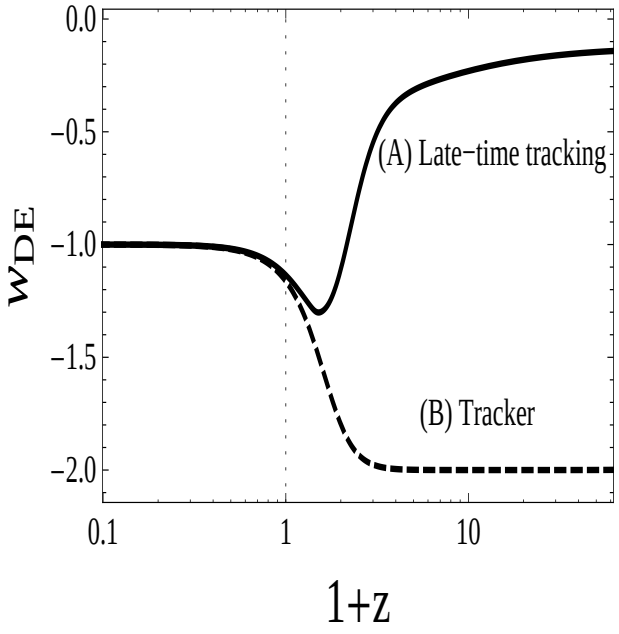

Figure 1: The equation of state $w_{\rm DE}$ versus the redshift z for the model parameters $\alpha = 1.37$ and $\beta = 0.44$ with two different initial conditions: (A) $r_1 = 0.03$, $r_2 = 0.003$, and (B) $r_1 = 0.999$, $r_2 = 7.0 \times 10^{-11}$. The case (B) corresponds to the tracker solution, whereas in the case (A) the solution approaches the tracker around today. The present epoch ($z = 0$) is shown as a dotted line (we also draw the dotted line in other figures).

During the deep matter era in which the field perturbation is negligibly small, the evolution of Ψ, Φ, δ, and V is similar to that in GR. The initial conditions are chosen to satisfy $\Phi' = 0$ and $\delta\varphi' = 0$. From Eqs. (60) and (61) this gives two constraints on the variables Φ, V, $\delta\varphi$, and δ. For given $\delta\varphi$ and δ, the initial conditions of Φ and V are determined accordingly. For the modes deep inside the Hubble radius, Eq. (46) provides a relation between $\delta\varphi$ and δ. We choose the initial condition $\delta = 10^{-5}$, but this can be chosen to be any value (as long as the amplitudes of perturbations do not matter). We note that the relation (46) cannot be used for the wavelengths larger than the Hubble radius. Apart from the modes deep inside the Hubble radius at the onset of integration, we adopt the initial condition $\delta\varphi = 0$. Provided that $\delta\varphi$ is small initially, the dynamics of perturbations is similar to that in the case $\delta\varphi = 0$. For large initial values of $\delta\varphi$, the field perturbation tends to oscillate for small-scales modes (associated with large wave numbers k). This situation is similar to what happens in the generalized Galileon model [20].

We identify the present epoch (the redshift $z = 0$) to be $\Omega_{\rm DE} = 0.72$. In order to find the evolution of the quantity $k/(aH)$, we also integrate the following equation

$$b' = b\,(1 + H'/H)\ , \tag{64}$$

where $b \equiv aH$. The scales relevant to the linear regime of the galaxy power spectrum are $30 \lesssim k/(a_0 H_0) \lesssim 600$, where the subscript "0" represents present values. Note that the above upper limit corresponds to $k = 0.2\,h\,{\rm Mpc}^{-1}$, where $h = 0.72 \pm 0.08$ [48]. For the scales $k/(a_0 H_0) \gtrsim 600$ the nonlinear effect becomes crucially important. Meanwhile, the wave numbers relevant to the ISW effect in CMB anisotropies correspond to the large-scale modes with $k/(a_0 H_0) = \mathcal{O}(1)$.

In Ref. [40] two of the present authors placed observational constraints on the Galileon model (1) from the background expansion history of the Universe. The combined data analysis of the type Ia supernovae (Constitution and Union2 sets), the CMB shift parameters (WMAP7), and the baryon acoustic oscillations (BAO) show that the tracker solution described by Eq. (23) is not favored, but the solutions that approach the tracker at late times can be compatible with the background observational constraints. As illustrated in Fig. 1, the equation of state $w_{\rm DE}$ for the tracker [case (B)] evolves from -2 (deep matter era) to -1 (dS epoch). The solution (A) in Fig. 1 starts to evolve from the value $w_{\rm DE} = -1/8$ and then it enters the tracking regime around the present epoch. In the flat FLRW background the best-fit model parameters are $\alpha = 1.411 \pm 0.056$, $\beta = 0.422 \pm 0.022$ (Constitution+CMB+BAO, 68 % CL), and $\alpha = 1.404 \pm 0.057$, $\beta = 0.419 \pm 0.023$ (Union2+CMB+BAO, 68 % CL).

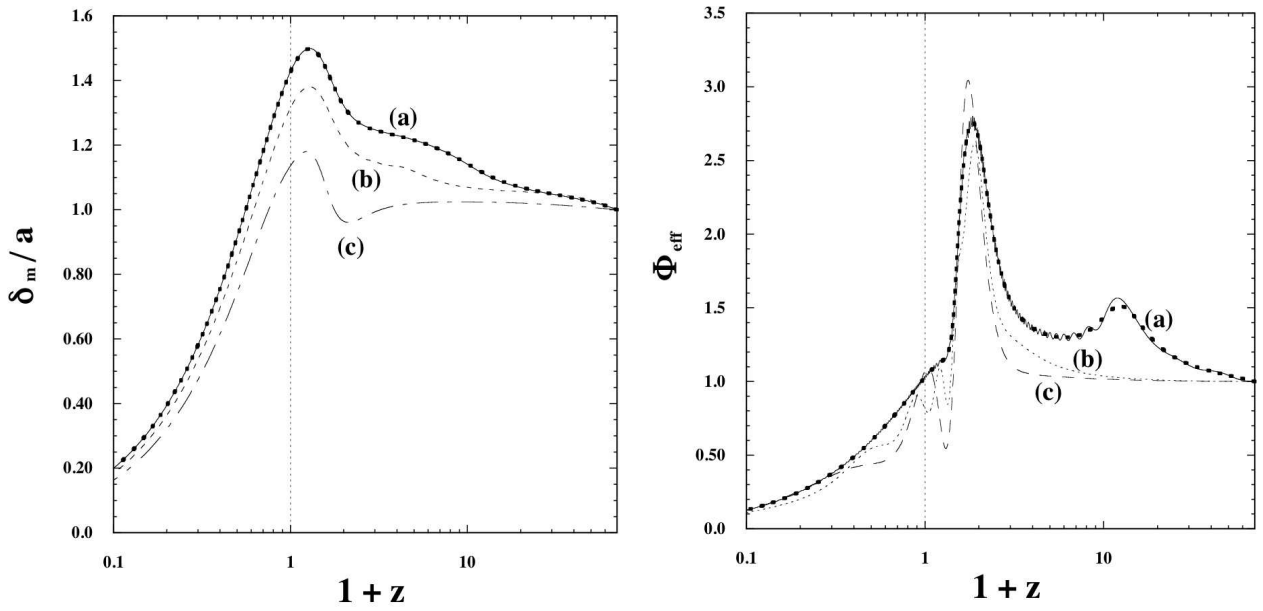

Figure 2: Evolution of the perturbations for $\alpha = 1.37$ and $\beta = 0.44$ with the background initial conditions $r_1 = 0.03$ and $r_2 = 0.003$ (corresponding to the case (A) of Fig. 1). (Left) δ_m/a versus z for the wave numbers (a) $k = 300a_0H_0$, (b) $k = 30a_0H_0$, and (c) $k = 5a_0H_0$. (Right) $\Phi_{\rm eff}$ versus z for the wave numbers (a) $k = 300a_0H_0$, (b) $k = 10a_0H_0$, and (c) $k = 5a_0H_0$. Note that δ_m/a and $\Phi_{\rm eff}$ are divided by their initial amplitudes $\delta_m(t_i)/a(t_i)$ and $\Phi_{\rm eff}(t_i)$, respectively, so that their initial values are normalized to be 1. The bold dotted lines show the results obtained under the quasi-static approximation on sub-horizon scales. The choice of initial conditions for perturbations is explained in the text.

A. Case of late-time tracking solutions

Let us consider the evolution of perturbations for the late-time tracking solutions. In Fig. 2 we plot δ_m/a and $\Phi_{\rm eff}$ versus the redshift z with the model parameters and initial conditions corresponding to the case (A) of Fig. 1. For the mode $k = 300a_0H_0$ we find that the full numerical result shows excellent agreement with that obtained under the quasi-static approximation on sub-horizon scales. The difference starts to appear for the modes $k/(a_0H_0) < \mathcal{O}(10)$. The left panel of Fig. 2 shows that, on larger scales, the growth of δ_m tends to be less significant. For the modes $k \gg a_0H_0$ the matter perturbation evolves faster than a during the matter era (i.e. faster than in the case of GR, $\delta_m \propto a$). The growth of δ_m/a turns into decrease after the Universe enters the epoch of cosmic acceleration.

In Fig. 3 we show the evolution of the growth index γ defined by [49]

$$\delta_m'/\delta_m = (\Omega_m)^\gamma\,. \tag{65}$$

The case (A) in Fig. 3 corresponds to the same model parameters and initial conditions as those given in the numerical simulations of Fig. 2. Unlike the ΛCDM model in which γ is nearly constant ($\simeq 0.55$ [50]) in the low redshift regime $0 < z < 1$, the variation of γ is significant for the solutions that approach the tracker at late times. Moreover the growth index today for the mode $k = 300a_0H_0$ is $\gamma_0 = 0.35$, which is quite different from that in the ΛCDM. For the wave lengths relevant to large-scale structures we find that the growth index today exhibits almost no dispersion with respect to k. This property is different from viable $f(R)$ dark energy models in which γ_0 can be dispersed [51]. If we choose smaller initial values of r_1 (i.e. the later tracking), we find that γ_0 tends to be smaller, e.g., $\gamma_0 = 0.23$ for the initial conditions $r_1 = 0.01$, $r_2 = 0.003$ with the model parameters $\alpha = 1.37$, $\beta = 0.44$.[4]

The right panel of Fig. 2 shows that, unlike the ΛCDM model, the effective gravitational potential $\Phi_{\rm eff}$ changes in time even during the matter era for the modes $k \gg aH$. This can be understood as follows. For the initial conditions corresponding to the late-time tracking solutions the effective gravitational coupling $G_{\rm eff}$ and the anisotropic parameter η are given by Eqs. (52) and (53), respectively, before reaching the tracker. Since $G_{\rm eff}/G \simeq 1 + 255\beta r_2/8 > 1$ and

[4] For the dark energy models with constant $w_{\rm DE}$ and γ, the current observations still allow the large parameter space of γ ranging from 0.2 to 0.6. [52].

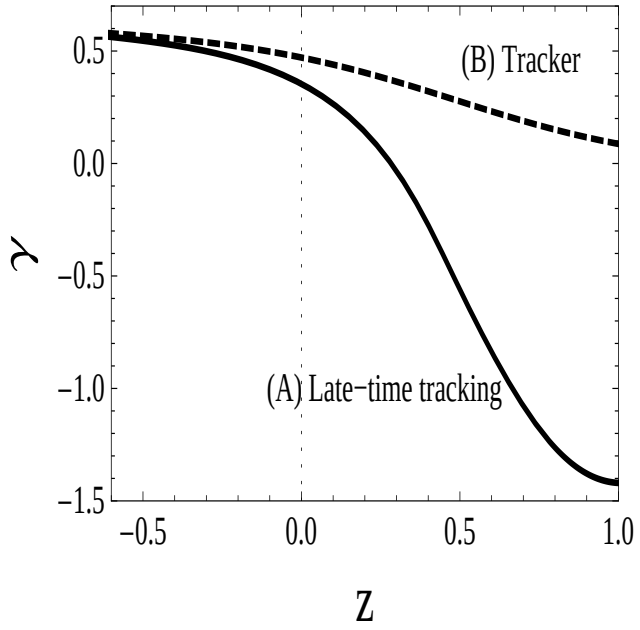

Figure 3: Variation of the growth index γ of matter perturbations for $\alpha = 1.37$ and $\beta = 0.44$ with the mode $k = 300 a_0 H_0$. The initial conditions of r_1 and r_2 for the cases (A) and (B) are the same as those given in the caption of Fig. 1.

$\eta \simeq 1 + 129\beta r_2/8 > 1$ in this regime, we have the larger growth rates of $\Phi_{\rm eff}$ and δ_m relative to those in GR. In particular the term $(G_{\rm eff}/G)(1+\eta)/2$ in Eq. (50) is larger than 1, which leads to the additional growth of $\Phi_{\rm eff}$ to that coming from δ_m. Note that in $f(R)$ gravity [46] and in Brans-Dicke theory [47] one has $(G_{\rm eff}/G)(1+\eta)/2 = 1$, so that the evolution of δ_m is directly related with the variation of $\Phi_{\rm eff}$. In Galileon gravity the unusual behavior of the anisotropic parameter η leads to the non-trivial evolution of perturbations. For the model parameters $\alpha = 1.37$ and $\beta = 0.44$, Eq. (56) gives $G_{\rm eff} \simeq 0.68G$ at the dS fixed point. As we see in Fig. 2, $\Phi_{\rm eff}$ begins to decrease at some point after the matter era.

For the large-scale modes relevant to the ISW effect in CMB anisotropies, i.e. $k/(a_0 H_0) \lesssim 10$, the effective gravitational potential is nearly constant in the early matter-dominated epoch, see the cases (b) and (c) in the right panel of Fig. 2. However, $\Phi_{\rm eff}$ exhibits temporal growth during the transition from the matter era to the epoch of cosmic acceleration. Note that in the ΛCDM model $\Phi_{\rm eff}$ decays without the temporal growth after the matter era. The characteristic variation of $\Phi_{\rm eff}$ in the Galileon model should leave observational signatures in CMB anisotropies as the ISW effect.

The above numerical results correspond to the fixed values of α and β ($\alpha = 1.37$, $\beta = 0.44$). If we use the bounds $\alpha = 1.404 \pm 0.057$, $\beta = 0.419 \pm 0.023$ constrained by Union2+CMB+BAO data sets, the effective gravitational coupling at the dS point is restricted in the range $0.5G < G_{\rm eff} < 0.72G$. The bounds coming from Constitution+CMB+BAO data give the similar constraint, i.e. $0.5G < G_{\rm eff} < 0.71G$. For the model parameters close to the upper limit $\alpha = 2\beta + 2/3$ of the allowed parameter space (i.e. $G_{\rm eff}$ is close to $0.5G$ at the dS point), the parameter η tends to show a divergence during the transition from the matter era to the dS epoch. If $G_{\rm eff}$ is larger than $0.66G$, we find that such divergent behavior can be typically avoided.

For the parameters α and β constrained observationally, the values of γ_0 are usually less than 0.4 for the late-time tracking with the minimum values of $w_{\rm DE}$ larger than -1.3. In addition the later tracking leads to smaller values of γ_0 with larger variations of γ. This property of the Galileon model can be clearly distinguished from the ΛCDM model.

B. Case of early-time tracking solutions

If the solutions are already close to the tracker in the early matter-dominated epoch, the evolution of perturbations is different from that discussed above. For the tracker one has $r_2 \propto a^6$ during the matter dominance, which is much faster than the evolution $r_2 \propto a^{3/8}$ in the regime $r_1 \ll 1$ and $r_2 \ll 1$. This means that r_2 is very much smaller than 1 for the redshift $z \gtrsim 1$. Then the second terms on the r.h.s. of Eqs. (54) and (55) are suppressed relative to the first

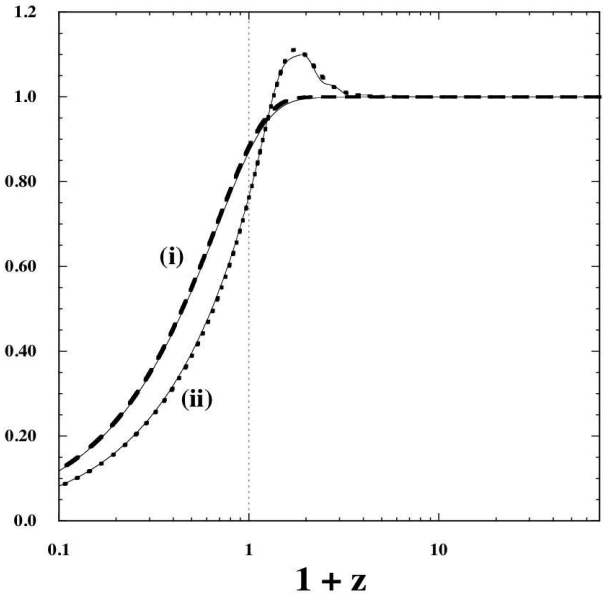

Figure 4: Evolution of (i) δ_m/a and (ii) $\Phi_{\rm eff}$ versus z for $\alpha = 1.37$ and $\beta = 0.44$ with the initial conditions $r_1 = 0.999$ and $r_2 = 7.0 \times 10^{-11}$ (corresponding to the case (B) of Fig. 1). Both δ_m/a and $\Phi_{\rm eff}$ are divided by their initial amplitudes. In this case the background cosmological solution is on the tracker from the onset of integration. The solid line shows the evolution of perturbations for the mode $k = 5a_0H_0$, whereas the bold dotted line represents the result derived under the quasi-static approximation on sub-horizon scales.

terms until recently. In Fig. 4 we plot the variation of δ_m/a and $\Phi_{\rm eff}$ for $\alpha = 1.37$ and $\beta = 0.44$ with the background initial conditions corresponding to the case (B) in Fig. 1. The solid line shows the evolution of perturbations for the mode $k = 5a_0H_0$, whereas the dotted line corresponds to the result derived under the quasi-static approximation on sub-horizon scales. In this case the evolution of the large-scale mode with $k = 5a_0H_0$ is similar to that for the modes deep inside the Hubble radius.

Figure 4 shows that the growth of matter perturbations in the deep matter era is almost identical to that in the ΛCDM model. In the regime $r_1 \simeq 1$ and $r_2 \ll 1$ one has $G_{\rm eff}/G \simeq 1 + 3.2r_2$ and $\eta \simeq 1 - 3.7r_2$, both of which are very close to 1. Recall that at the dS point $G_{\rm eff}/G \simeq 0.68$ and $\eta = 1$. Since η is very close to 1 and $G_{\rm eff}$ is different from G only around the dS solution, the evolution of perturbations is milder than that corresponding to the late-time tracking solutions. The case (B) of Fig. 3 shows γ versus z for the mode $k = 300a_0H_0$ with the initial condition corresponding to the tracker solution. In this case the growth index today is found to be $\gamma_0 \simeq 0.47$ with the variation of γ in the low-redshift regime. In Fig. 4 we also find the small temporal growth of $\Phi_{\rm eff}$ from the end of the matter era to the epoch of cosmic acceleration. This can also give rise to a non-negligible contribution to the ISW effect in CMB anisotropies. We recall, however, that the tracker solution is not favored at the background level by the joint analysis of observational data.

C. Case of $\alpha = \beta = 0$

Let us finally consider the model in which only the terms up to $\mathcal{L}_3$ are present, i.e. $\alpha = \beta = 0$. Although such a model is disfavored observationally, it is of interest to study what happens for the evolution of perturbations due to the peculiar divergence of $G_{\rm eff}$ at the dS point (which occurs along the line $\alpha = 2\beta$).

First of all we have numerically found that the late-time tracking behavior as in the case (A) of Fig. 1 is not easy to be realized even by choosing many different initial conditions. This is the main reason why the combined data analysis at the background level do not favor such model parameters. For $\alpha = \beta = 0$ one has $\eta = 1$ independent of the values of r_1 and r_2, whereas $G_{\rm eff} \simeq G$ for $r_1 \ll 1, r_2 \ll 1$ and $G_{\rm eff} \simeq 1 + r_2/4$ for $r_1 = 1, r_2 \ll 1$.

In Fig. 5 we plot the variation of δ_m/a and $\Phi_{\rm eff}$ with the initial conditions $r_1 = 0.05$ and $r_2 = 0.001$ for two different wave numbers: $k = 300a_0H_0$ and $k = 5a_0H_0$. In this simulation the solution reaches the tracker region ($r_1 \simeq 1$) around the redshift $z = 5$, e.g., $r_1 = 0.99$ and $r_2 = 4.14 \times 10^{-4}$ at $z = 5.34$. Hence the evolution of perturbations for $z \gtrsim 5$ is similar to that in the ΛCDM model. The effective gravitational coupling $G_{\rm eff}$ increases with the growth of r_2

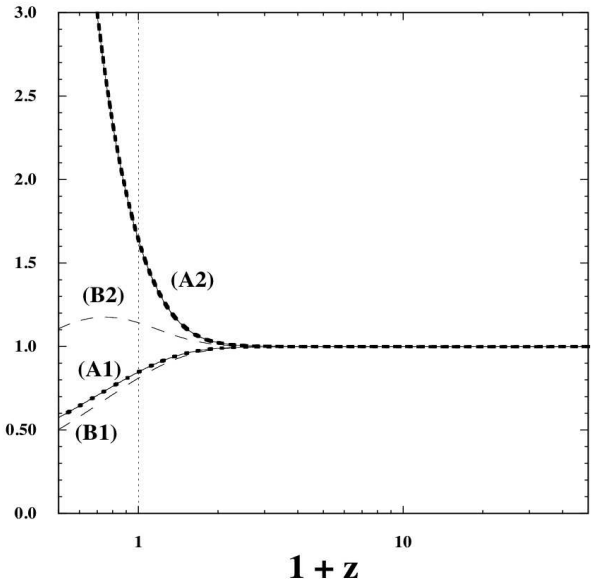

Figure 5: Evolution of perturbations for $\alpha = 0$ and $\beta = 0$ with the initial conditions $r_1 = 0.05$ and $r_2 = 0.001$. Each line corresponds to (A1) δ_m/a for the mode $k = 300a_0H_0$, (A2) $\Phi_{\rm eff}$ for the mode $k = 300a_0H_0$, (B1) δ_m/a for the mode $k = 5a_0H_0$, and (B2) $\Phi_{\rm eff}$ for the mode $k = 5a_0H_0$. Both δ_m/a and $\Phi_{\rm eff}$ are divided by their initial amplitudes. The bold dotted lines correspond to the results obtained under the quasi-static approximation on sub-horizon scales.

for $z \lesssim 5$. In this case the numerical value of $G_{\rm eff}$ today is $G_{\rm eff} \simeq 1.94G$ with $r_2 \simeq 0.72$. For the mode $k = 300a_0H_0$ the growth index today is found to be $\gamma_0 \simeq 0.43$, which is smaller than the value in the ΛCDM model.

In Fig. 5 the effective gravitational potential for the mode $k = 300a_0H_0$ grows around the present epoch in spite of the decrease of δ_m/a. This can be understood by the fact that the term $(G_{\rm eff}/G)(1+\eta)/2$, which is equivalent to $G_{\rm eff}/G$ for $\alpha = \beta = 0$, continues to grow toward the dS solution. While the decrease of the density parameter Ω_m overwhelms the increase of $G_{\rm eff}/G$ in Eq. (51) for matter perturbations, the presence of the additional term $(aH/k)^2$ in Eq. (50) stimulates the growth of $\Phi_{\rm eff}$ around today. Numerically we find that the growth of $\Phi_{\rm eff}$ eventually turns into the decrease in future as δ_m decays sufficiently (which is not shown in Fig. 5). For $k = 5a_0H_0$ the growth of $\Phi_{\rm eff}$ around today is milder relative to the modes deep inside the Hubble radius.

The anti-correlation between δ_m/a and $\Phi_{\rm eff}$ seen in Fig. 5 is similar to the one found in the generalized Galileon model [20]. This anti-correlation mainly comes from the fact that $G_{\rm eff}/G$ continues to grow toward the dS point and that the parameter η does not become smaller than 1 to compensate the growth of $G_{\rm eff}/G$ (unlike $f(R)$ gravity and Brans-Dicke theory). In the numerical simulations of Fig. 2 the effective gravitational coupling is larger than G in the regime $r_1 \ll 1$ and $r_2 \ll 1$, but it finally approaches the asymptotic value $G_{\rm eff} \simeq 0.68G$. In this case both δ_m/a and $\Phi_{\rm eff}$ start to decay by today, whose property is different from that in the case $\alpha = \beta = 0$. Since the observational constraints on α and β do not allow the region close to the line $\alpha = 2\beta$, the anti-correlation between δ_m/a and $\Phi_{\rm eff}$ does not typically occur for the viable model parameters.

VI. CONCLUSIONS

We have studied the dynamics of cosmological perturbations in the Galileon model whose Lagrangian satisfies the Galilean symmetry $\partial_\mu\phi \to \partial_\mu\phi + b_\mu$ in the flat space-time. In this theory there exists stable dS solutions with $\dot{\phi} =$ constant. In the deep matter era the General Relativistic behavior can be recovered because of a small field velocity, but the Universe finally enters the epoch of cosmic acceleration after the growth of $\dot{\phi}$.

Before reaching the dS attractor, the solutions approach a tracker characterized by $r_1 = 1$ (i.e. the evolution $\dot{\phi} \propto H^{-1}$). The tracking epoch depends on the initial conditions of the background cosmological variables. The combined data analysis based on the background expansion history of the Universe (SN Ia+CMB shift parameters+BAO) favor the late-time tracking around today. This corresponds to the initial conditions $r_1 \ll 1$ and $r_2 \ll 1$ in the deep matter era, so that r_1 approaches 1 in the low-redshift regime ($z \lesssim 1$).

The study about the evolution of cosmological perturbations can allow us to distinguish the Galileon model from the ΛCDM model further. In the presence of a non-relativistic perfect fluid, we have derived full perturbation equations

for the model described by the action (1). In spite of their complexities it is possible to obtain simpler equations for the matter perturbation δ_m and the effective gravitational potential $\Phi_{\rm eff}$ under a quasi-static approximation on sub-horizon scales.

The two important quantities associated with the growth of δ_m and $\Phi_{\rm eff}$ are the effective gravitational coupling $G_{\rm eff}$ and the anisotropic parameter $\eta = -\Phi/\Psi$. In three distinct regimes we have approximately derived the expressions of $G_{\rm eff}$ and η, see Eqs. (52)-(57). For the initial conditions that lead to the late-time tracking behavior, the solutions start from the regime $r_1 \ll 1$, $r_2 \ll 1$ with positive β (which is required to avoid ghosts). In this regime Eqs. (52) and (53) show that $G_{\rm eff}/G \simeq 1 + 255\beta r_2/8 > 1$ and $\eta \simeq 1 + 129\beta r_2/8 > 1$. This gives rise to the larger growth rates of δ_m and $\Phi_{\rm eff}$ relative to those in the ΛCDM model.

In $f(R)$ gravity and Brans-Dicke theory the anisotropic parameter η is less than 1, so that the combination $(G_{\rm eff}/G)(1+\eta)/2$ remains to be 1. In the Galileon model the fact that $\eta > 1$ in the regime $r_1 \ll 1$, $r_2 \ll 1$ leads to the further growth of $\Phi_{\rm eff}$ for sub-horizon modes. At the dS fixed point we have that $G_{\rm eff}/G = 1/[3(\alpha - 2\beta)]$ and $\eta = 1$. For the parameters of α and β observationally constrained at the background level [40],the effective gravitational coupling $G_{\rm eff}$ is smaller than $0.72G$. Then the perturbations δ_m/a and $\Phi_{\rm eff}$ turn into decrease around today, as we see in the numerical simulation of Fig. 2.

For the solutions that approach the tracker at the early epoch of the matter era, $G_{\rm eff}$ and η are approximately given by Eqs. (54) and (55), respectively, in the regime $r_1 = 1, r_2 \ll 1$. Since the evolution of r_2 in the tracking regime is very fast ($r_2 \propto a^6$), the correction term βr_2 to $G_{\rm eff}$ and η becomes important around the present epoch in which r_2 grows to the order of 1. Hence the deviation from the ΛCDM model for the evolution of δ_m and $\Phi_{\rm eff}$ appears only at late times, as we see in Fig. 4. The early tracking behavior is however disfavored from joint observational constraints at the background level.

For the late-time tracking solutions we have found that the growth index γ of matter perturbations rapidly changes in the low-redshift regime [as in the case (A) of Fig. 3]. The values of γ today on the scales relevant to large-scale structures are typically smaller than 0.4 for the model parameters constrained by the observations at the background level. As the tracking occurs at a later epoch, the presents values of γ tend to be smaller. On large scales relevant to the ISW effect in CMB anisotropies the effective gravitational potential $\Phi_{\rm eff}$ exhibits a temporal growth around the present epoch. It will be of interest to constrain the Galileon model further from the combined data analysis of large-scale structures, CMB, and weak lensing.

ACKNOWLEDGEMENTS

The work of A. D. F. and S. T. was supported by the Grant-in-Aid for Scientific Research Fund of the JSPS Nos. 10271 and 30318802. S. T. also thanks financial support for the Grant-in-Aid for Scientific Research on Innovative Areas (No. 21111006). S. T. is grateful to Bin Wang for warm hospitality during his stay in Shanghai Jiao Tong University.

Appendix A: Bianchi identities

We confirm the consistency of perturbation equations by using the Bianchi identities. We write the action (1) in the form

$$S = \int {\rm d}^4x\sqrt{-g}\,\mathcal{L}\,, \tag{A1}$$

where $\mathcal{L}$ is the total Lagrangian. Variation of the action (A1) with respect to $g_{\alpha\beta}$ gives

$$\delta S = \int {\rm d}^4x\sqrt{-g}\,\Sigma^{\alpha\beta}\delta g_{\alpha\beta}\,. \tag{A2}$$

Then the Bianchi identities lead to

$$\nabla_\beta \Sigma^{\alpha\beta} = \partial_\beta \Sigma^{\alpha\beta} + \Gamma^\alpha_{\lambda\beta}\Sigma^{\lambda\beta} + \Gamma^\beta_{\lambda\beta}\Sigma^{\alpha\lambda} = 0\,, \tag{A3}$$

where $\Gamma^\alpha_{\lambda\beta}$ is the Christoffel symbol.

We perturb Eq. (A3) at first order. Then we find

$$\partial_\beta \delta\Sigma^{\alpha\beta} + \Gamma^\alpha_{\lambda\beta}\delta\Sigma^{\lambda\beta} + \Gamma^\beta_{\lambda\beta}\delta\Sigma^{\alpha\lambda} = 0\,, \tag{A4}$$

where we have used the fact that the background equation satisfies $\Sigma^{\alpha\beta}=0$. For the case $\alpha=0$ we have

$$\partial_0\delta\Sigma^{00}+\partial_i\delta\Sigma^{0i}+\Gamma^0_{\lambda\beta}\delta\Sigma^{\lambda\beta}+\Gamma^\beta_{0\beta}\delta\Sigma^{00}+\Gamma^\beta_{i\beta}\delta\Sigma^{0i}=0\,. \tag{A5}$$

Using the relations $\Gamma^0_{00}=0$, $\Gamma^0_{0i}=0$, $\Gamma^0_{ij}=a^2H\delta_{ij}$, $\Gamma^i_{00}=0$, $\Gamma^i_{0j}=H\delta_{ij}$, $\Gamma^i_{jk}=0$, Eq. (A5) reduces to

$$\partial_0\delta\Sigma^{00}+\partial_i\delta\Sigma^{0i}+a^2H\sum_i\delta\Sigma^{ii}+3H\delta\Sigma^{00}=0\,. \tag{A6}$$

In our Galileon model the condition (A6) leads to the following relation

$$E_1\equiv\dot{E}_\Psi+3HE_\Psi-HE_\Phi-\frac{k^2}{a^2}E_\chi=0\,, \tag{A7}$$

where E_Ψ corresponds to Eq. (32), E_Φ to Eq. (33), and E_χ to Eq. (34). Combining Eq. (35) with Eq. (A7) and inserting the background equations of motion, we find

$$E_1-\dot{\phi}E_{\delta\phi}=\rho_m\left(\frac{k^2}{a^2}\chi-3\dot{\Phi}-\frac{k^2}{a^2}v-\dot{\delta}\right)=0\,, \tag{A8}$$

which matches with Eq. (28) for $w=0$.

Equation (37) can be also derived from the spatial part of the Bianchi identities. It follows that

$$\dot{E}_\chi+3HE_\chi-\frac{1}{3}E_\Phi=\frac{1}{3}\frac{k^2}{a^2}\tilde{E}_\gamma=0\,, \tag{A9}$$

where $\tilde{E}_\gamma$ corresponds to Eq. (37).

Appendix B: Coefficients of perturbation equations

In this Appendix we show the coefficients of the perturbation equations (32), (33), (34), and (35).

Eq. (32)

$$A_1=6HM_{\rm pl}^2-3c_3\dot{\phi}^3/M^3+45c_4H\dot{\phi}^4/M^6-63c_5H^2\dot{\phi}^5/M^9\,, \tag{B1}$$
$$A_2=c_2\dot{\phi}-9c_3H\dot{\phi}^2/M^3+90c_4H^2\dot{\phi}^3/M^6-105c_5H^3\dot{\phi}^4/M^9\,, \tag{B2}$$
$$A_3=2M_{\rm pl}^2+3c_4\dot{\phi}^4/M^6-6c_5H\dot{\phi}^5/M^9\,, \tag{B3}$$
$$A_4=2\rho_m-9H^2M_{\rm pl}^2-c_1M^3\phi/2-3c_2\dot{\phi}^2/2+15c_3H\dot{\phi}^3/M^3-315c_4H^2\dot{\phi}^4/(2M^6)+189c_5H^3\dot{\phi}^5/M^9\,, \tag{B4}$$
$$A_5=-2HM_{\rm pl}^2+c_3\dot{\phi}^3/M^3-15c_4H\dot{\phi}^4/M^6+21c_5H^2\dot{\phi}^5/M^9\,, \tag{B5}$$
$$A_6=-c_3\dot{\phi}^2/M^3+12c_4H\dot{\phi}^3/M^6-15c_5H^2\dot{\phi}^4/M^9\,. \tag{B6}$$

Eq. (33)

$$B_1=3A_3\,, \tag{B7}$$
$$B_2=3A_6\,, \tag{B8}$$
$$B_3=18HM_{\rm pl}^2+27c_4H\dot{\phi}^4/M^6+36c_4\dot{\phi}^3\ddot{\phi}/M^6-54c_5H^2\dot{\phi}^5/M^9-90c_5H\dot{\phi}^4\ddot{\phi}/M^9-18c_5\dot{H}\dot{\phi}^5/M^9\,, \tag{B9}$$
$$\begin{aligned}B_4=&-3c_2\dot{\phi}-6c_3\dot{\phi}\ddot{\phi}/M^3+36c_4\dot{H}\dot{\phi}^3/M^6+108c_4H\dot{\phi}^2\ddot{\phi}/M^6+54c_4H^2\dot{\phi}^3/M^6\\&-90c_5H^3\dot{\phi}^4/M^9-180c_5H^2\dot{\phi}^3\ddot{\phi}/M^9-90c_5H\dot{H}\dot{\phi}^4/M^9\,,\end{aligned} \tag{B10}$$
$$B_5=-A_1\,, \tag{B11}$$
$$B_6=2M_{\rm pl}^2-c_4\dot{\phi}^4/M^6-6c_5\dot{\phi}^4\ddot{\phi}/M^9\,, \tag{B12}$$
$$B_7=12c_4\dot{\phi}^2\ddot{\phi}/M^6+4c_4H\dot{\phi}^3/M^6-6c_5\dot{H}\dot{\phi}^4/M^9-6c_5H^2\dot{\phi}^4/M^9-24c_5H\dot{\phi}^3\ddot{\phi}/M^9\,, \tag{B13}$$
$$B_8=A_3\,, \tag{B14}$$
$$\begin{aligned}B_9=&-9H^2M_{\rm pl}^2-6\dot{H}M_{\rm pl}^2-3\rho_m+3c_1M^3\phi/2+3c_2\dot{\phi}^2/2+9c_3\dot{\phi}^2\ddot{\phi}/M^3-135c_4H^2\dot{\phi}^4/(2M^6)\\&-180c_4H\dot{\phi}^3\ddot{\phi}/M^6-45c_4\dot{H}\dot{\phi}^4/M^6+315c_5H^2\dot{\phi}^4\ddot{\phi}/M^9+126c_5H^3\dot{\phi}^5/M^9+126c_5H\dot{H}\dot{\phi}^5/M^9\,,\end{aligned} \tag{B15}$$
$$B_{10}=-A_3\,, \tag{B16}$$
$$B_{11}=-2HM_{\rm pl}^2-3c_4H\dot{\phi}^4/M^6-12c_4\dot{\phi}^3\ddot{\phi}/M^6+6c_5\dot{H}\dot{\phi}^5/M^9+30c_5H\dot{\phi}^4\ddot{\phi}/M^9+6c_5H^2\dot{\phi}^5/M^9\,. \tag{B17}$$

Eq. (34)

$$C_1 = A_3\,, \qquad C_2 = A_6\,, \qquad C_3 = -A_1/3\,, \tag{B18}$$

$$C_4 = -c_2\dot\phi + 3c_3H\dot\phi^2/M^3 - 18c_4H^2\dot\phi^3/M^6 + 15c_5H^3\dot\phi^4/M^9\,. \tag{B19}$$

Eq. (35)

$$D_1 = 3A_6\,, \tag{B20}$$

$$D_2 = c_2 - 6c_3H\dot\phi/M^3 + 54c_4H^2\dot\phi^2/M^6 - 60c_5H^3\dot\phi^3/M^9\,, \tag{B21}$$

$$\begin{aligned} D_3 = {} & 3c_2\dot\phi - 18c_3H\dot\phi^2/M^3 - 6c_3\dot\phi\ddot\phi/M^3 + 108c_4H\dot\phi^2\ddot\phi/M^6 + 162c_4H^2\dot\phi^3/M^6 + 36c_4\dot H\dot\phi^3/M^6 \\ & -90c_5(H\dot H\dot\phi^4/M^9 + 2H^3\dot\phi^4/M^9 + 2H^2\dot\phi^3\ddot\phi/M^9)\,, \end{aligned} \tag{B22}$$

$$\begin{aligned} D_4 = {} & 3c_2H - 6c_3\dot H\dot\phi/M^3 - 18c_3H^2\dot\phi/M^3 - 6c_3H\ddot\phi/M^3 + 162c_4H^3\dot\phi^2/M^6 + 108c_4H\dot H\dot\phi^2/M^6 \\ & +108c_4H^2\dot\phi\ddot\phi/M^6 - 180c_5(H^3\dot\phi^2\ddot\phi/M^9 + H^2\dot H\dot\phi^3/M^9 + H^4\dot\phi^3/M^9)\,, \end{aligned} \tag{B23}$$

$$D_5 = -A_2\,, \tag{B24}$$

$$D_6 = -A_6\,, \tag{B25}$$

$$D_7 = B_7\,, \tag{B26}$$

$$\begin{aligned} D_8 = {} & 3c_1M^3/2 + 3c_2\ddot\phi + 9c_2H\dot\phi - 27c_3H^2\dot\phi^2/M^3 - 18c_3H\dot\phi\ddot\phi/M^3 - 9c_3\dot H\dot\phi^2/M^3 + 162c_4H^2\dot\phi^2\ddot\phi/M^6 \\ & +162c_4H^3\dot\phi^3/M^6 + 108c_4H\dot H\dot\phi^3/M^6 - 180c_5H^3\dot\phi^3\ddot\phi/M^9 - 135c_5(H^2\dot H\dot\phi^4/M^9 + H^4\dot\phi^4/M^9)\,, \end{aligned} \tag{B27}$$

$$\begin{aligned} D_9 = {} & c_2 - 4c_3H\dot\phi/M^3 - 2c_3\ddot\phi/M^3 + 26c_4H^2\dot\phi^2/M^6 + 12c_4\dot H\dot\phi^2/M^6 + 24c_4H\dot\phi\ddot\phi/M^6 \\ & -36c_5H^2\dot\phi^2\ddot\phi/M^9 - 24c_5(H^3\dot\phi^3/M^9 + H\dot H\dot\phi^3/M^9)\,, \end{aligned} \tag{B28}$$

$$D_{10} = A_6\,, \tag{B29}$$

$$\begin{aligned} D_{11} = {} & c_1M^3/2 - 3c_2H\dot\phi - c_2\ddot\phi + 27c_3H^2\dot\phi^2/M^3 + 18c_3H\dot\phi\ddot\phi/M^3 + 9c_3\dot H\dot\phi^2/M^3 - 180c_4H\dot H\dot\phi^3/M^6 \\ & -270c_4(H^2\dot\phi^2\ddot\phi/M^6 + H^3\dot\phi^3/M^6) + 420c_5H^3\dot\phi^3\ddot\phi/M^9 + 315c_5(H^4\dot\phi^4/M^9 + H^2\dot H\dot\phi^4/M^9)\,, \end{aligned} \tag{B30}$$

$$\begin{aligned} D_{12} = {} & -c_2\dot\phi + 4c_3H\dot\phi^2/M^3 + 2c_3\dot\phi\ddot\phi/M^3 - 30c_4H^2\dot\phi^3/M^6 - 36c_4H\dot\phi^2\ddot\phi/M^6 - 12c_4\dot H\dot\phi^3/M^6 \\ & +30c_5(H\dot H\dot\phi^4/M^9 + H^3\dot\phi^4/M^9 + 2H^2\dot\phi^3\ddot\phi/M^9)\,. \end{aligned} \tag{B31}$$

[1] E. J. Copeland, M. Sami and S. Tsujikawa, Int. J. Mod. Phys. D **15**, 1753 (2006); R. Durrer and R. Maartens, Gen. Rel. Grav. **40**, 301 (2008); V. A. Rubakov and P. G. Tinyakov, Phys. Usp. **51**, 759 (2008) [arXiv:0802.4379 [hep-th]]; T. P. Sotiriou and V. Faraoni, Rev. Mod. Phys. **82**, 451 (2010); A. De Felice and S. Tsujikawa, Living Rev. Rel. **13**, 3 (2010).

[2] S. Capozziello, Int. J. Mod. Phys. D **11**, 483 (2002); S. Capozziello, S. Carloni and A. Troisi, Recent Res. Dev. Astron. Astrophys. **1**, 625 (2003); S. Capozziello, V. F. Cardone, S. Carloni and A. Troisi, Int. J. Mod. Phys. D **12**, 1969 (2003); S. M. Carroll, V. Duvvuri, M. Trodden and M. S. Turner, Phys. Rev. D **70**, 043528 (2004).

[3] L. Amendola, Phys. Rev. D **60**, 043501 (1999); J. P. Uzan, Phys. Rev. D **59**, 123510 (1999); T. Chiba, Phys. Rev. D **60**, 083508 (1999); N. Bartolo and M. Pietroni, Phys. Rev. D **61** 023518 (2000); F. Perrotta, C. Baccigalupi and S. Matarrese, Phys. Rev. D **61**, 023507 (2000).

[4] S. M. Carroll *et al.,* Phys. Rev. D **71**, 063513 (2005); S. Nojiri, S. D. Odintsov and M. Sasaki, Phys. Rev. D **71**, 123509 (2005); G. Calcagni, S. Tsujikawa and M. Sami, Class. Quant. Grav. **22**, 3977 (2005); A. De Felice, M. Hindmarsh and M. Trodden, JCAP **0608**, 005 (2006). I. Navarro and K. Van Acoleyen, Phys. Lett. B **622**, 1 (2005); I. Navarro and K. Van Acoleyen, JCAP **0603**, 008 (2006); A. De Felice and T. Suyama, JCAP **0906**, 034 (2009); A. De Felice and T. Suyama, arXiv:1010.3886; A. De Felice and T. Tanaka, Prog. Theor. Phys. **124**, 503 (2010).

[5] G. R. Dvali, G. Gabadadze and M. Porrati, Phys. Lett. B **485**, 208 (2000).

[6] A. Nicolis, R. Rattazzi and E. Trincherini, Phys. Rev. D **79**, 064036 (2009).

[7] L. Amendola, R. Gannouji, D. Polarski and S. Tsujikawa, Phys. Rev. D **75**, 083504 (2007); B. Li and J. D. Barrow, Phys. Rev. D **75**, 084010 (2007); L. Amendola and S. Tsujikawa, Phys. Lett. B **660**, 125 (2008); W. Hu and I. Sawicki, Phys. Rev. D **76**, 064004 (2007); A. A. Starobinsky, JETP Lett. **86**, 157 (2007); S. A. Appleby and R. A. Battye, Phys. Lett. B **654**, 7 (2007); S. Tsujikawa, Phys. Rev. D **77**, 023507 (2008); E. V. Linder, Phys. Rev. D **80**, 123528 (2009).

[8] A. A. Starobinsky, Phys. Lett. B **91**, 99 (1980).

[9] J. Khoury and A. Weltman, Phys. Rev. Lett. **93**, 171104 (2004); Phys. Rev. D **69**, 044026 (2004).

[10] J. A. R. Cembranos, Phys. Rev. D **73**, 064029 (2006); I. Navarro and K. Van Acoleyen, JCAP **0702**, 022 (2007); T. Faulkner, M. Tegmark, E. F. Bunn and Y. Mao, Phys. Rev. D **76**, 063505 (2007); S. Capozziello and S. Tsujikawa, Phys. Rev. D **77**, 107501 (2008).

[11] A. I. Vainshtein, Phys. Lett. B **39**, 393 (1972).

[12] C. Deffayet, G. R. Dvali, G. Gabadadze and A. I. Vainshtein, Phys. Rev. D **65**, 044026 (2002); M. Porrati, Phys. Lett. B **534**, 209 (2002).

[13] A. Nicolis and R. Rattazzi, JHEP **0406**, 059 (2004); K. Koyama and R. Maartens, JCAP **0601**, 016 (2006); D. Gorbunov, K. Koyama and S. Sibiryakov, Phys. Rev. D **73**, 044016 (2006).

[14] M. Fairbairn and A. Goobar, Phys. Lett. B **642**, 432 (2006); R. Maartens and E. Majerotto, Phys. Rev. D **74**, 023004 (2006); U. Alam and V. Sahni, Phys. Rev. D **73**, 084024 (2006); Y. S. Song, I. Sawicki and W. Hu, Phys. Rev. D **75**, 064003 (2007); J. Q. Xia, Phys. Rev. D **79**, 103527 (2009).

[15] C. Deffayet, G. Esposito-Farese and A. Vikman, Phys. Rev. D **79**, 084003 (2009); C. Deffayet, S. Deser and G. Esposito-Farese, Phys. Rev. D **80**, 064015 (2009).

[16] A. De Felice and S. Tsujikawa, Phys. Rev. Lett. **105**, 111301 (2010).

[17] A. De Felice and S. Tsujikawa, arXiv:1008.4236 [hep-th].

[18] N. Chow and J. Khoury, Phys. Rev. D **80**, 024037 (2009).

[19] F. P. Silva and K. Koyama, Phys. Rev. D **80**, 121301 (2009).

[20] T. Kobayashi, H. Tashiro and D. Suzuki, Phys. Rev. D **81**, 063513 (2010).

[21] T. Kobayashi, Phys. Rev. D **81**, 103533 (2010).

[22] C. de Rham and A. J. Tolley, JCAP **1005**, 015 (2010).

[23] R. Gannouji and M. Sami, Phys. Rev. D **82**, 024011 (2010).

[24] A. De Felice and S. Tsujikawa, JCAP **1007**, 024 (2010).

[25] A. De Felice, S. Mukohyama and S. Tsujikawa, Phys. Rev. D **82**, 023524 (2010).

[26] P. Creminelli, A. Nicolis and E. Trincherini, arXiv:1007.0027 [hep-th].

[27] A. Padilla, P. M. Saffin and S. Y. Zhou, arXiv:1007.5424 [hep-th]; arXiv:1008.0745 [hep-th].

[28] C. Deffayet, S. Deser and G. Esposito-Farese, arXiv:1007.5278 [gr-qc].

[29] C. Deffayet, O. Pujolas, I. Sawicki and A. Vikman, JCAP **1010**, 026 (2010).

[30] T. Kobayashi, M. Yamaguchi and J. Yokoyama, arXiv:1008.0603 [hep-th].

[31] K. Hinterbichler, M. Trodden and D. Wesley, arXiv:1008.1305 [hep-th].

[32] A. Ali, R. Gannouji and M. Sami, arXiv:1008.1588 [astro-ph.CO].

[33] M. Andrews, K. Hinterbichler, J. Khoury and M. Trodden, arXiv:1008.4128 [hep-th].

[34] G. L. Goon, K. Hinterbichler and M. Trodden, arXiv:1008.4580 [hep-th].

[35] S. Mizuno and K. Koyama, arXiv:1009.0677 [hep-th].

[36] C. Burrage, C. de Rham, D. Seery and A. J. Tolley, arXiv:1009.2497 [hep-th].

[37] E. Babichev, arXiv:1009.2921 [hep-th].

[38] S. Y. Zhou, arXiv:1011.0863 [hep-th].

[39] R. Kimura and K. Yamamoto, arXiv:1011.2006 [astro-ph.CO].

[40] S. Nesseris, A. De Felice and S. Tsujikawa, arXiv:1010.0407 [astro-ph.CO].

[41] C. Schimd, J. P. Uzan and A. Riazuelo, Phys. Rev. D **71**, 083512 (2005); M. Ishak, A. Upadhye and D. N. Spergel, Phys. Rev. D **74**, 043513 (2006); L. Knox, Y. S. Song and J. A. Tyson, Phys. Rev. D **74**, 023512 (2006); D. Huterer and E. V. Linder, Phys. Rev. D **75**, 023519 (2007); P. Zhang, M. Liguori, R. Bean and S. Dodelson, Phys. Rev. Lett. **99**, 141302 (2007); S. Wang, L. Hui, M. May and Z. Haiman, Phys. Rev. D **76**, 063503 (2007); B. Jain and P. Zhang, Phys. Rev. D **78**, 063503 (2008); S. F. Daniel, R. R. Caldwell, A. Cooray and A. Melchiorri, Phys. Rev. D **77**, 103513 (2008); E. Bertschinger and P. Zukin, Phys. Rev. D **78**, 024015 (2008); G. B. Zhao, L. Pogosian, A. Silvestri and J. Zylberberg, Phys. Rev. D **79**, 083513 (2009); Y. S. Song and K. Koyama, JCAP **0901**, 048 (2009); Y. S. Song and O. Dore, JCAP **0903**, 025 (2009); S. A. Thomas, F. B. Abdalla and J. Weller, Mon. Not. Roy. Astron. Soc. **395**, 197 (2009); J. Guzik, B. Jain and M. Takada, Phys. Rev. D **81**, 023503 (2010); P. Brax, C. van de Bruck, A. C. Davis and D. Shaw, JCAP **1004**, 032 (2010); R. Bean and M. Tangmatitham, Phys. Rev. D **81**, 083534 (2010); G. B. Zhao *et al.*, Phys. Rev. D **81**, 103510 (2010); S. F. Daniel *et al.,* Phys. Rev. D **81**, 123508 (2010); R. Gannouji *et al.,* arXiv:1010.3769 [astro-ph.CO].

[42] J. M. Bardeen, Phys. Rev. D **22**, 1882 (1980).

[43] A. De Felice, J. M. Gerard and T. Suyama, Phys. Rev. D **81**, 063527 (2010); Phys. Rev. D **82**, 063526 (2010).

[44] J. c. Hwang and H. Noh, Phys. Rev. D **71**, 063536 (2005).

[45] A. A. Starobinsky, JETP Lett. **68**, 757 (1998); B. Boisseau, G. Esposito-Farese, D. Polarski and A. A. Starobinsky, Phys. Rev. Lett. **85**, 2236 (2000).

[46] S. Tsujikawa, Phys. Rev. D **76**, 023514 (2007); S. Tsujikawa, K. Uddin and R. Tavakol, Phys. Rev. D **77**, 043007 (2008).

[47] S. Tsujikawa, K. Uddin, S. Mizuno, R. Tavakol and J. Yokoyama, Phys. Rev. D **77**, 103009 (2008).

[48] W. J. Percival *et al.*, Astrophys. J. **657**, 645 (2007).

[49] J. Peebles, *The large-scale structure of the universe*, Princeton University Press (1980).

[50] L. M. Wang and P. J. Steinhardt, Astrophys. J. **508**, 483 (1998).

[51] S. Tsujikawa, R. Gannouji, B. Moraes and D. Polarski, Phys. Rev. D **80**, 084044 (2009).

[52] D. Rapetti, S. W. Allen, A. Mantz and H. Ebeling, arXiv:0911.1787 [astro-ph.CO].